

# Photoprotons from Be, C, and O\*

L. COHEN, A. K. MANN, B. J. PATTON, K. REIBEL,<sup>†</sup> W. E. STEPHENS, AND E. J. WINHOLD  
*Physics Department, University of Pennsylvania, Philadelphia, Pennsylvania*

(Received June 25, 1956)

The photoprotons ejected from thin foils of beryllium, carbon, and polyethylene and from oxygen gas by 25-Mev betatron bremsstrahlung were observed in nuclear emulsions with good resolution. The energy distributions and yields of photoprotons were determined for Be, C, and O. Excitation functions for transitions to the ground states of the residual nuclei have been constructed from the observed photoproton energy distributions of C and O. Structure is observed in the proton energy distributions and hence appears in the corresponding  $(\gamma, p)$  excitation functions. This structure is in rough agreement with that observed in  $(\gamma, n)$  reactions in C and O.

## INTRODUCTION

A PRINCIPAL feature of photonuclear transmutations is the "giant resonance" region of photon absorption. Since the photoneutron and photoproton yields<sup>1</sup> in this region seem to exhaust the dipole sum rule<sup>2</sup> (in medium atomic weight nuclei), this resonance is ascribed to an electric dipole absorption. The photon energy (at least in medium weight nuclei) is soon distributed over the nuclear particles and an evaporation<sup>3</sup> of a neutron or proton takes place.

In light nuclei, the nuclear levels are more widely spaced and in some cases the residual nucleus can be left in only a few possible levels. In such cases it is sometimes possible to identify specific transitions and to observe the character of the intermediate excited states thus obtaining detailed information concerning the photon absorption. In those nuclei in which the giant resonance width is less than the spacing of the residual nucleus states, the use of heterogeneous bremsstrahlung photons still allows an identification of the transition by the observation of the photoproton energy. With these objectives in mind we have measured the photoprotons from the light elements beryl-

lium,<sup>4</sup> carbon,<sup>5</sup> and oxygen.<sup>6</sup> Similar investigations have been reported independently by Spicer<sup>7</sup> and Johansson and Forlsman<sup>8</sup> both of whom studied the photodisintegration of oxygen at somewhat lower bremsstrahlung energies than were used in the present work.

Several experiments<sup>9</sup> have indicated fine structure in the "giant resonance" absorption by light elements. Our experiments offer independent evidence of this fine structure and additional information on the details of these levels.

## EXPERIMENTAL PROCEDURE

A well-collimated bremsstrahlung photon beam from a 25-Mev betatron irradiates either a foil or gas target and the photoprotons which are ejected are recorded in nuclear emulsion plates placed at 90° to the beam. The experimental arrangement has been described in previous papers.<sup>3,10</sup> The photoproton tracks are scanned with a Spencer binocular microscope at a magnification

TABLE I. Exposure data.

Element Target	Be Beryllium foil	C (1st run) Graphite slab	C (2nd run) Polyethylene sheet	O Oxygen gas
Thickness (mg/cm <sup>2</sup> )	5.8	6.3	1.97	2.1
Betatron energy (Mev)	23.5	24	24	25
Roentgens at foil	11 500	17 300	10 900	22 400
Emulsion type (Ilford)	C2X2	C2X2	C2	C2X2
Emulsion thickness (microns)	100	100	100	200
Area scanned (cm <sup>2</sup> )	0.285	0.338	0.63	0.36
Tracks measured	781	441	873	1123

TABLE II. Calibration data (energies in Mev).

Reaction	Q value <sup>a</sup>	$E_{45 \text{ scale}}$	$E_{\text{corr}}^b$	$E_{\text{obs}}^c$	Half-width
$\text{N}^{14}(d, p)\text{N}^{15}$	8.609	9.10	8.92	8.96	0.23
$\text{C}^{13}(d, p)\text{C}^{14}$	5.994	6.50	6.28	6.38	0.21
$\text{C}^{12}(d, p)\text{C}^{13}$	2.723	3.40	3.07	3.12	0.22

<sup>a</sup> F. Ajzenberg and T. Lauritsen, *Revs. Modern Phys.* **27**, 77 (1955).

<sup>b</sup> Corrected for passing through 200-microgram/cm<sup>2</sup> gold foil target backing and 3.42-mg/cm<sup>2</sup> aluminum window.

<sup>c</sup> Based on range energy curve for C2X2 Ilford emulsions given by Lees, Morrison, and Rosser, *Proc. Phys. Soc. (London)* **A66**, 13 (1953).

<sup>4</sup> L. Cohen, M.S. thesis, University of Pennsylvania, 1956 (unpublished).

<sup>5</sup> W. E. Stephens and A. K. Mann, *Phys. Rev.* **98**, 241(A) (1955); K. Reibel, M.S. thesis, University of Pennsylvania, 1956 (unpublished).

<sup>6</sup> Stephens, Mann, Patton, and Winhold, *Phys. Rev.* **98**, 839 (1955); B. J. Patton, Ph.D. thesis, University of Pennsylvania, 1955 (unpublished).

<sup>7</sup> B. M. Spicer, *Phys. Rev.* **99**, 33 (1955).

<sup>8</sup> S. A. E. Johansson and B. Forlsman, *Phys. Rev.* **99**, 1031 (1955).

<sup>9</sup> Katz, Haslam, Horsley, Cameron, and Montalbetti, *Phys. Rev.* **95**, 464 (1954); A. S. Penfold and B. M. Spicer, *Phys. Rev.* **100**, 1377 (1955); Wright, Morrison, Reid, and Atkinson, *Proc. Phys. Soc. (London)* **A69**, 77 (1956).

<sup>10</sup> M. E. Toms and W. E. Stephens, *Phys. Rev.* **82**, 709 (1951); **92**, 362 (1953); **95**, 1209 (1954).

\* Supported in part by the joint program of the Office of Naval Research and U. S. Atomic Energy Commission and by the Air Research and Development Command.

<sup>†</sup> National Science Foundation Predoctoral Fellow, 1954-1956.

<sup>1</sup> A. K. Mann and J. Halpern, *Phys. Rev.* **82**, 733 (1951); R. Nathans and J. Halpern, *Phys. Rev.* **93**, 437 (1954); Montalbetti, Katz, and Goldemberg, *Phys. Rev.* **91**, 659 (1953).

<sup>2</sup> J. S. Levinger and H. A. Bethe, *Phys. Rev.* **78**, 115 (1950).

<sup>3</sup> P. R. Byerly and W. E. Stephens, *Phys. Rev.* **83**, 54 (1951).

of 970 times and the proton energies determined from the measured ranges. Table I shows the pertinent details relating to the various exposures. The roentgen doses were measured with an integrating ionization chamber calibrated against a Victoreen 100r thimble encased in an 8-cm Lucite cylinder. The betatron energy was determined from the maximum proton energy observed and the proton binding energy. Several of the plates used were Ilford C2 type diluted with gelatin by a factor 2 (designated C2X2) in order to reduce background. No apparent advantage was thereby gained.

In order to check both the range-energy calibration of the nuclear emulsions and to determine the resolution to be expected, we have exposed Ilford C2X2 emulsions to monochromatic protons from several  $(d,p)$  reactions induced in a 3 mg/cm<sup>2</sup> nylon foil by 800-kev deuterons from our statitron. The proton energies to be expected at 45° were calculated from the known  $Q$  values as given in Table II and these energies were corrected for the gold foil target backing and aluminum window through which the protons had to pass to reach the emulsions. The corrected energies are given in column 4 of Table II. The observed proton ranges were converted

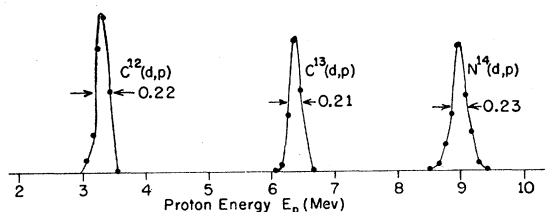


FIG. 1. Energy distribution of monoenergetic proton groups as observed in C2X2 nuclear emulsion.

to energy using the range-energy curve of Lees *et al.*<sup>11</sup> and are shown in Fig. 1. The good agreement ( $\sim 1\%$ ) between the observed mean energies and the calculated values is shown in Table II. From this calibration we believe the proton energies to be accurate to about 0.1 Mev. Figure 1 also indicates the limits to resolution, approximately 0.2 Mev, imposed primarily by range straggling in the emulsion. The only additional uncertainty in photoproton energy arises from target thickness corrections which for the higher energy protons are small in the oxygen run and in the second carbon run. Target thickness in beryllium and gas absorption in oxygen become limiting factors for photoprotons of less than 5 Mev.

The background from  $(n,p)$  reactions in the target and from neutron recoils in the top layer of the emulsion is estimated from observations to be small ( $\sim 1\%$ ) and of low energy ( $\sim 2$  Mev) and is therefore neglected.

<sup>11</sup> Lees, Morrison, and Rosser, Proc. Phys. Soc. (London) A66, 13 (1953).

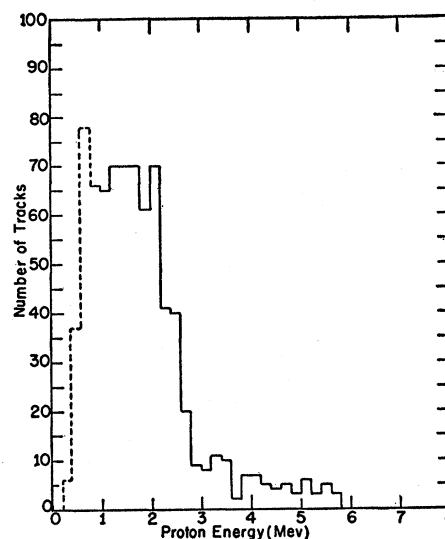


FIG. 2. Observed energy distribution of photoprotons from beryllium not corrected for target thickness.

## EXPERIMENTAL RESULTS

### Beryllium

Figure 2 shows the energy distribution of 781 tracks which appeared to come from the beryllium foil at angles relative to the incident beam between 45° and 135°. These tracks were corrected for recoil and their ranges increased by the equivalent of half the target thickness to give the distribution shown in Fig. 3. Below 2 Mev the half-target correction is inadequate and the dashed histogram is not a good indication of

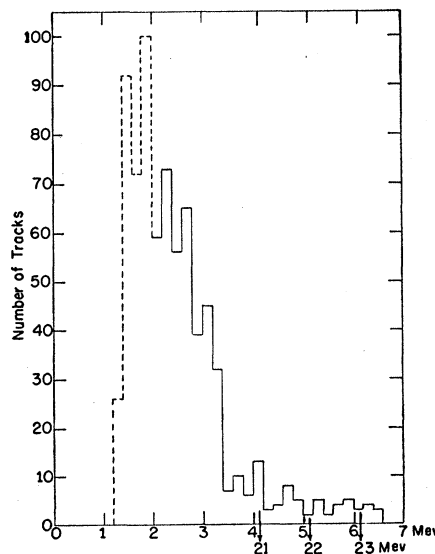


FIG. 3. Corrected energy distribution of photoprotons from beryllium. The upper energy scale is the disintegration energy. The lower scale is the photon energy if the recoil nucleus were left in its ground state.

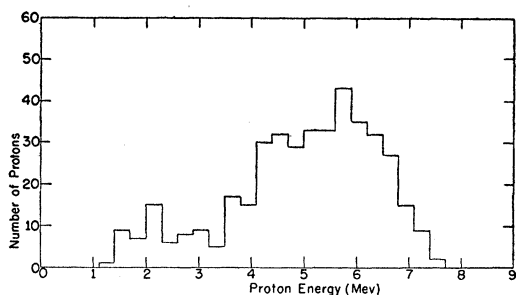


FIG. 4. Observed energy distribution of 408 photoprotons from the first run on carbon.

the true disintegration energy distribution. If we assume a photoproton energy distribution which is roughly constant from 0.5 to 3 Mev and correct it for target absorption, we obtain agreement with the observed data. This assumption is somewhat arbitrary at the lower energy end, the 0.5-Mev value having been chosen from Coulomb barrier considerations. On this basis we estimate that 30% of the photoprotons would not emerge from the beryllium foil and 10% of those emerging would not be detected because of short length in the emulsion. From these considerations we have corrected the observed yield of  $3.66 \times 10^4$  to  $(5.8 \pm 3) \times 10^4$  protons per mole per roentgen (assuming isotropic angular distribution).

It is energetically possible for deuterons as well as protons to be emitted in the photodisintegration of beryllium since the thresholds are 16.68 and 16.87 Mev respectively. We have looked for possible photodeuterons among the photoparticles by grain counting 66 tracks of length greater than 50 microns. The relatively short track lengths severely restricted the reliability of this measurement, but no evidence for photodeuterons was found.

### Carbon

The first carbon run was made using as a target the thinnest slab which we could grind from a graphite

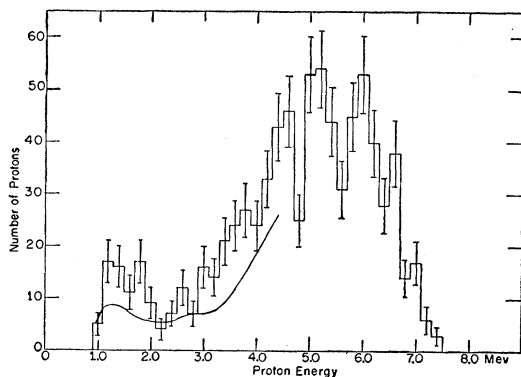


FIG. 5. Observed energy distribution of photoprotons from polyethylene (carbon second run) plotted in 0.2-Mev intervals. Smooth curve gives the proton distribution predicted from the inverse reaction  $B^{11}(p, \gamma)$  by applying detailed balancing.

plate. The carbon slab was approximately 2 mils thick and weighed  $6.3 \text{ mg/cm}^2$ . Figure 4 shows the photoproton energy distribution observed. This histogram is corrected for the half-target thickness but not for recoil. In an attempt to improve the energy resolution, which in this first carbon run was limited by target thickness to about 0.4 Mev, a second run was made using a polyethylene foil of about  $2 \text{ mg/cm}^2$  thickness. The results of this exposure are shown in Fig. 5 and show an appreciable improvement in resolution. The energy scale is the observed proton energy plus half the effective target thickness in Mev. There were 69 tracks which left the emulsion before stopping. These were added to the curve of Fig. 5 at an energy equal to the average of those tracks which stopped in the emulsion and which had a range longer than the one in question. Most of these were added above 6 Mev. It will be noted that the independent distributions of Figs. 4 and 5 are in substantial agreement except for difference in resolution.

The total yield was calculated (using the data of Table I) on the assumption that the foil was  $\text{CH}_2$ . Different scanned regions in the plate gave yields at  $90^\circ$  of  $13.2$ ,  $15.1$ ,  $12.4$ , and  $15.6 \times 10^4$  protons per mole per roentgen unit. A weighted average gives  $14.6 \times 10^4$  protons per mole per roentgen. The reliability may be estimated to be consistent with a 25% probable error. When corrected for angular distribution,<sup>12</sup> the yield is  $(12 \pm 3) \times 10^4$  protons per mole per roentgen unit.

### Oxygen

A gaseous target was chosen for the oxygen irradiation in order to eliminate the effects of other elements and to achieve a minimum of target thickness correction consistent with measurable yield. This was accomplished at a sacrifice of a localized target, introduced geometric corrections into the angular distributions, and necessitated correction for absorption in the oxygen gas. It is possible that inaccuracies in this latter correction reduced slightly the resolution to be expected. The gaseous absorption also introduces a cutoff for the detection of low-energy protons. Since long-range protons were expected because of the low binding energy

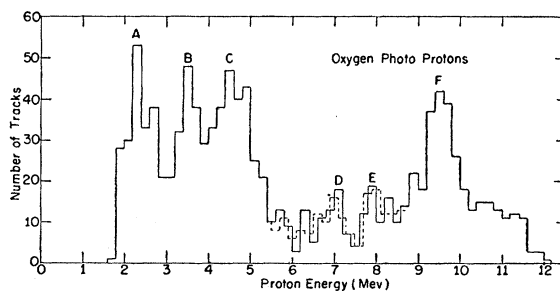


FIG. 6. Observed energy distribution of 1123 photoprotons from oxygen corrected for gas absorption.

<sup>12</sup> Halpern, Mann, and Rothman, Phys. Rev. **87**, 164 (1952).

of protons in oxygen (12.11 Mev), 200-micron emulsions were used in this run.

Three areas on the chosen plate were scanned. Area I was 5 mm from the emulsion edge nearest the incident beam and 227 tracks were found at  $90^\circ \pm 30^\circ$  in 0.086 cm<sup>2</sup> of plate. However, 18% of the tracks observed went through the emulsion and entered the glass backing. To improve the measurement of the higher energy protons, an additional 0.278 cm<sup>2</sup> at 3 cm from the edge was scanned. This scanning yielded 315 tracks at  $90^\circ \pm 30^\circ$  of which only 3% went out of the emulsion. In both these areas, the absorption of the oxygen gas was important for low-energy protons and especially important for those at angles greater than  $30^\circ$  to the plane normal to the beam. The oxygen absorption cut off low-energy protons at 1.3 and 1.8 Mev for angles greater than  $30^\circ$  in areas I and II respectively. To reduce this biasing effect, another area (III) was scanned closer to the edge in a less fogged plate.

The observed proton energy distribution from 1123 tracks found in areas I and II at angles  $30^\circ$  to  $150^\circ$  from the beam is plotted in Fig. 6. These tracks have been corrected for oxygen gas absorption and dip and the energies determined from the range-energy curve of Lees *et al.* Each track which left the emulsion was added to the curve at the average energy of those tracks longer than itself.

The yield can be calculated as  $10.7 \times 10^4$  protons per mole per roentgen unit for region I and  $11.5 \times 10^4$  for region II. The weighted average of these is  $11.2 \times 10^4$  protons per mole per roentgen at 25-Mev bremsstrahlung and is estimated to be accurate to about 20%. Angular distributions were determined for each of the proton peaks of Fig. 6. Poor statistics and uncertain geometrical corrections did not allow a definitive interpretation of the angular distribution of each peak. Nevertheless, the data seem to indicate isotropy for the protons of energy less than 6 Mev and a distribution peaked around  $90^\circ$  with possibly some forward shift for protons of greater than 6-Mev energy as shown in Fig. 7.

### Discussion

In order profitably to discuss the implications of the observed photoproton yields (summarized in Table III) and energy distributions presented in the previous sections, it is necessary to identify the energy of the photon whose absorption caused the emission of the photoproton. The continuous spectrum of the incident

TABLE III. Photoproton yields.

	Be	C	O
Betatron energy (Mev)	23.5	24	25
Photoproton yield (protons/mole roentgen)	$(5.8 \pm 3) \times 10^4$	$(12 \pm 3) \times 10^4$	$(11 \pm 3) \times 10^4$
Approximate integrated cross section (Mev-mb)	(32)	~60	~60
Dipole sum rule (Mev-mb)	190	250	340

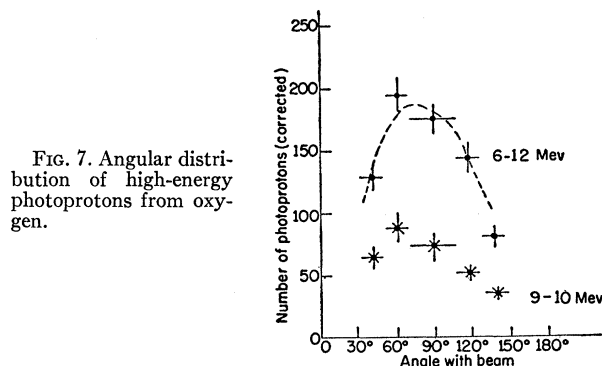


FIG. 7. Angular distribution of high-energy photoprotons from oxygen.

bremsstrahlung radiation and the possibility of leaving the residual nucleus in one of several states makes this difficult. (The level schemes and relations between photon and proton energies for the nuclei that have been studied are presented in Fig. 8.) Nevertheless, those protons which have energies greater than the difference between the maximum photon energy and the threshold energy for transitions to the first excited state of the residual nucleus must be associated with transitions to the ground state. From this part of the photoproton energy spectrum it is then possible, with a knowledge of the bremsstrahlung spectrum, to construct a partial curve of cross section *versus* photon energy for the process of photoproton emission leading to the ground state of the residual nucleus. The rest of the photoproton energy distribution can be translated to an excitation curve only if additional information is available or if simplifying assumptions are made.

**Beryllium.**—The observed beryllium photoproton yield of  $5.8 \times 10^4$  protons per mole per roentgen at 23.5-Mev bremsstrahlung energy is considerably greater than the value of  $(1.8 \pm 0.6) \times 10^4$  reported previously by Mann and Halpern.<sup>13</sup> The difference is due to an incorrect estimate of the large absorption of the low-energy protons in the rather thick targets of the latter experiment.

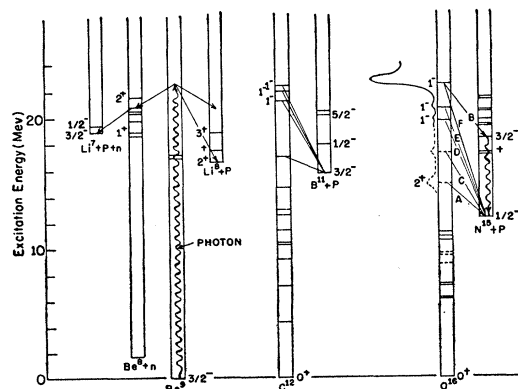


FIG. 8. Level schemes and transitions associated with the photoprotons from beryllium, carbon, and oxygen.

<sup>13</sup> A. K. Mann and J. Halpern, Phys. Rev. 82, 733 (1951).

Haslam *et al.*<sup>14</sup> report a yield of the radioactivity of  $\text{Li}^8$  from  $\text{Be}^9(\gamma, p)\text{Li}^8$  of  $2.34 \times 10^4$  lithium-eight nuclei per mole per roentgen unit at 24 Mev. Haslam also gives a cross-section curve for this reaction from which an integrated cross section of 13 Mev-mb is deduced for the giant resonance whose peak is located at 22 Mev. If we assume that the photoproton emission cross section has a similar shape, then we can estimate from our photoproton yield an integrated cross section for photoprotons of 32 Mev mb. This value, however, includes contributions from both the  $\text{Be}^9(\gamma, p)\text{Li}^8$  and  $\text{Be}^9(\gamma, np)\text{Li}^7$  reactions.

Nathans and Halpern<sup>15</sup> have measured the excitation function for photoneutron emission from beryllium and deduce a cross section curve which has peaks at 10 Mev and 22 Mev. The 10-Mev peak can only be produced by  $\text{Be}^9(\gamma, n)$  because of energy considerations. The 22-Mev peak may arise from both  $\text{Be}^9(\gamma, n)\text{Be}^8$  and  $\text{Be}^9(\gamma, np)\text{Li}^7$  and has an integrated cross section of 15 Mev mb. The level schemes of  $\text{Li}^7$  and  $\text{Be}^8$  (see Fig. 8) make it seem reasonable that much of this 15 Mev-mb is due to  $\text{Be}^9(\gamma, np)\text{Li}^7$ . The integrated cross section for photoproton emission will be the sum of the  $\text{Be}^9(\gamma, p)\text{Li}^8$  and  $\text{Be}^9(\gamma, np)\text{Li}^7$  cross sections, i.e., of the order of 28 Mev-mb, assuming that most of the 22-Mev photoneutron resonance is  $\text{Be}^9(\gamma, np)$ . Our measured value of 32 Mev mb is in reasonable agreement with that value.

The energy distribution of the beryllium photoprotons (Fig. 3) shows very few protons of energy greater than 4 Mev, implying that transitions to the ground and first excited states of  $\text{Li}^8$  are relatively rare. The presence of many low-energy protons is consistent with the suggestion made above that a significant fraction of the observed photoprotons are associated with transitions from  $\text{Be}^8$  levels to  $\text{Li}^7$  following neutron emission from  $\text{Be}^9$ .

**Carbon.**—The carbon photoproton yield of  $(12 \pm 3) \times 10^4$  protons per mole per roentgen unit is slightly lower than the value of  $(18 \pm 3) \times 10^4$  obtained from counter measurements by Halpern and Mann.<sup>16</sup> The difference is probably associated with an over-correction for target absorption of photoprotons in the latter value. Using our measured energy distribution, it is possible to recorrect the counter data for target absorption and obtain a yield of  $9.5 \times 10^4$  in satisfactory agreement with the present result.

In analyzing the energy distribution data of Fig. 5, it must be noted that protons of energies less than 5.4 Mev can be produced not only in transitions to the ground state of  $\text{B}^{11}$ , but also in transitions to the first excited state of  $\text{B}^{11}$  at 2.14 Mev. Likewise, protons of energy less than 2.7 Mev can be produced also in transi-

tions to the 4.46 and 5.03 Mev levels of  $\text{B}^{11}$  (see Fig. 8). Interpretation of the portion of the proton spectrum below 5.4 Mev is thus not clear. We can however, utilize information on the cross section of the inverse reaction  $\text{B}^{11}(p, \gamma)\text{C}^{12}$  leading directly to the  $\text{C}^{12}$  ground state by applying the principle of detailed balance. The absolute  $90^\circ$  cross section for production of the "16"-Mev capture gamma ray leaving the  $\text{C}^{12}$  in its ground state was obtained by correcting the high-energy proton data of Bair *et al.*<sup>17</sup> for channel width and resolution and normalizing them to the low-energy proton absolute data of Huus and Day.<sup>18</sup> The smooth curve of Fig. 5 is the expected energy distribution of photoprotons ejected by the bremsstrahlung photons leaving the  $\text{B}^{11}$  in its ground state as calculated from the inverse reaction data using detailed balance. This curve has roughly the same shape as our experimental spectrum although the number of protons is somewhat less. The uncertainty in each curve in the region 3 to 5 Mev is of the order of 25% so that the discrepancy is within the experimental errors. The fraction of the protons in the energy region below 5 Mev produced in transitions to the excited states of  $\text{B}^{11}$  can be estimated very roughly from the difference between the two curves as one-fourth. This is not the same as the fraction of photon absorptions which result in transitions to the excited states since, for instance, the fraction of photon absorptions between 21.4 and 23.4 Mev which go to the first excited state is obtained (in principle) by subtracting the ground state protons (determined from detailed balancing) between 3.0 and 3.9 Mev from all those observed in this region and comparing with the observed protons in the region between 5.0 and 5.9 Mev. In this fashion the fraction of photon absorption in the giant resonance region with proton emission which results in transition to the first excited state compared to the ground state can be estimated very roughly to be  $\frac{1}{4}$  to  $\frac{1}{5}$ . Phase space and penetrability factors account for a ratio of  $\frac{1}{3}$ . This value may be lowered to about  $\frac{1}{5}$  by reduced width considerations.<sup>19</sup> Using the simplifying assumption that all of the protons are associated with transitions to the ground state of  $\text{B}^{11}$ , we transform the proton energy distribution of Fig. 5 into a cross-section curve (shown in Fig. 9) for photon absorption with emission of photoprotons at  $90^\circ$  to the photon beam. This will be inexact to the extent of the transitions to the excited states of  $\text{B}^{11}$ . Any protons which leave  $\text{B}^{11}$  in the 2.14-Mev excited state should be associated with a photon energy 2.14 Mev greater and hence would be multiplied by a larger bremsstrahlung factor. This would increase the cross section in the region of the peak. The smooth curve in Fig. 9 is the cross section for photoproton emission leaving  $\text{B}^{11}$  in its ground state as predicted by detail balance from the  $\text{B}^{11}(p, \gamma)$  cross section. The circle

<sup>14</sup> Haslam, Katz, Crosby, Summers-Gill, and Cameron, Can. J. Phys. **31**, 210 (1953).

<sup>15</sup> R. Nathans and J. Halpern, Phys. Rev. **92**, 940 (1953).

<sup>16</sup> J. Halpern and A. K. Mann, Phys. Rev. **83**, 370 (1951). The energy distribution assumed in this reference for the carbon photoprotons in order to correct for target absorption was peaked lower than the actual distribution which is shown in Fig. 5.

<sup>17</sup> Bair, Kingston, and Willard, Phys. Rev. **100**, 21 (1955).

<sup>18</sup> T. Huus and R. B. Day, Phys. Rev. **91**, 599 (1953).

<sup>19</sup> Mann, Stephens, and Wilkinson, Phys. Rev. **97**, 1184 (1955).

represents an absolute value of  $C^{12}(\gamma, p)$  measured at 17.63-Mev gamma-ray energy by Mann and Titterton.<sup>20</sup>

The integrated cross section deduced from Fig. 9 is about 56 Mev mb. The apparent numbers of protons of energy less than 5.3 Mev which are produced in transitions to the excited states of  $B^{11}$  could increase the integrated cross section (because of the different bremsstrahlung factor) by possibly 5 to 10 Mev mb.

A striking feature of the data is the fine structure in the proton energy distribution of Fig. 5 which is reflected in the cross-section curve of Fig. 9. Resonances occur with some certainty at 21.5 and 22.6 Mev and possibly also at 20.8 and 23.1 Mev. The 17.3-Mev group appears to correspond in location and approximate magnitude to the broad  $1^-$  or  $2^+$  state<sup>21</sup> at 17.22 Mev in  $C^{12}$  found by proton capture in  $B^{11}$ . Interpretation of the 20.8-Mev peak is not certain. It is most probably a resonance to the  $B^{11}$  ground state, although it may partly be associated with photon absorption at about 23 Mev followed by transition to the first excited state of  $B^{11}$ . If one assumes transitions to the  $B^{11}$  ground state, the integrated cross sections for the resonances at 17.3, 20.8, 21.5, and 22.6 Mev are roughly 2, 6, 9, and 12 Mev mb. Our resolution is such that each of these may well consist of narrower unresolved levels.

The giant resonance is generally ascribed primarily to electric dipole absorption of the incident radiation by the target nucleus. Since the ground state of  $C^{12}$  is  $0^+$ , such absorption can lead only to  $1^-$  excited states in  $C^{12}$  which may decay by the emission of protons to  $B^{11}$  or neutrons to  $C^{11}$ . The latter are mirror nuclei with similar low-lying states whose spins and parities makes them accessible to transitions from the  $1^-$  states in  $C^{12}$ . (The binding energy of a neutron in  $C^{12}$  is 18.71 Mev so no states in  $C^{12}$  below this excitation energy will be associated with the emission of neutrons.) It is to be expected that fine structure in the excitation function for  $C^{12}(\gamma, p)B^{11}$  will be approximately similar to that for  $C^{12}(\gamma, n)C^{11}$  which has been determined from betatron excitation yield measurements.<sup>9</sup> The latter method is apparently of greater resolution than is available in the proton work but there is rough agreement in the location and magnitude of the resonances observed in the photoproton reactions with those observed in the photoneutron reaction in  $C^{12}$ . It should be emphasized that the experimental uncertainties involved in both measurements are considerable and prevent precise comparison; nevertheless, it appears that the proton energy distribution and the inferred cross-section curve may be interpreted as providing independent confirming evidence of structure in the giant resonance in  $C^{12}$ .

*Oxygen.*—It will be seen that the energy distribution of Fig. 6 contains several clearly delineated proton

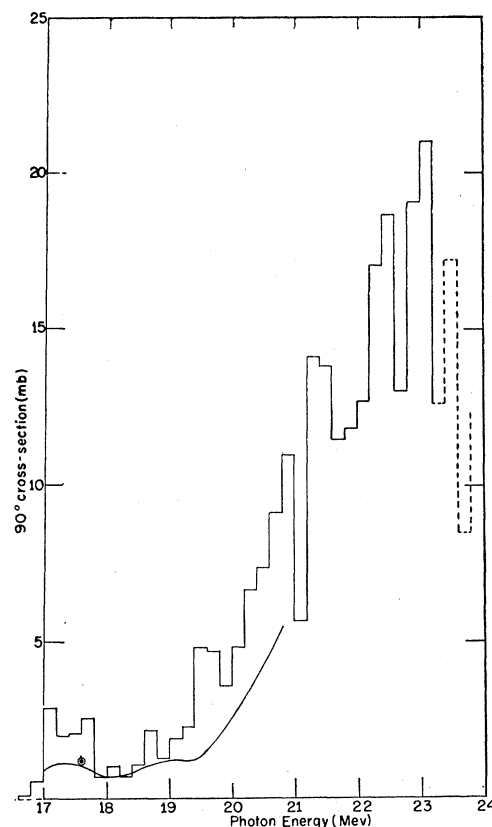


Fig. 9. Photon absorption cross-section curve for the ejection of photoprotons from carbon obtained from Fig. 5 on the assumption that the resultant  $B^{11}$  nucleus is always left in its ground state. This curve gives an upper limit to the cross section for photon energies below about 20.5 Mev and a lower limit for higher energies. The curve is uncertain above photon energies of 23 Mev because of statistical uncertainties and corrections. The smooth curve is the cross section predicted from  $B^{11}(p, \gamma)$  data by detailed balancing. The point at 17.6 Mev is due to Mann and Titterton, reference 20.

groups which have been labeled alphabetically. Groups D, E, and F can consist only of protons emitted in transitions to the  $\frac{1}{2}^-$  ground state of  $N^{15}$  because transitions to higher states would not produce protons of energy greater than 6.5 Mev. Therefore, each of these groups must correspond to a resonance in the photon absorption cross section. This part of the proton energy distribution can then be transformed into a cross section curve for ground-state transitions as shown in Fig. 10. The large peak at 22.4 Mev comprises a major fraction of the giant resonance and presumably results from excitation of  $O^{16}$  into one or more  $1^-$  states. The smaller peaks appear to be partially resolved resonances at 19.6 and 20.6 Mev. The integrated cross sections are approximately 20 Mev mb for the larger peak and 2 Mev-mb for each of the smaller ones. The measurements of Katz *et al.*<sup>22</sup> of the  $O^{16}(\gamma, n)O^{15}$  yield curve

<sup>20</sup> A. K. Mann and E. W. Titterton (to be published).

<sup>21</sup> H. E. Gove and E. G. Paul, Phys. Rev. 97, 104 (1955).

<sup>22</sup> Katz, Haslam, Horsley, Cameron, and Montalbetti, Phys. Rev. 95, 464 (1954).

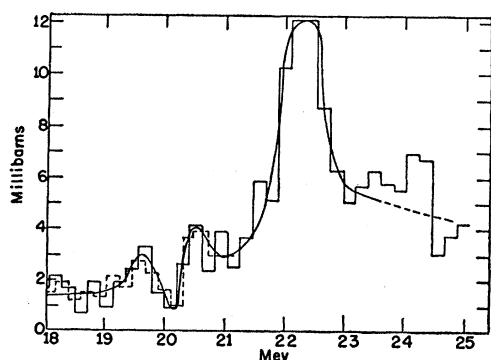


FIG. 10. Photon absorption cross-section curve for the ejection of photoprotons from oxygen obtained from Fig. 6 on the assumption that the resultant  $N^{15}$  nucleus is left in its ground state.

indicate a strong resonance at 21.9 Mev of estimated integrated cross section 7.5 Mev mb and smaller resonances (each approximately 2 Mev mb) at 19.3 and 20.7 Mev. More recently, Penfold and Spicer<sup>23</sup> have found indications of a larger number of closely spaced levels in  $O^{16}(\gamma, n)O^{15}$ . Although these closely spaced resonances are not resolved in the photoproton work, nevertheless, as in  $C^{12}$ , there seems to be rough agreement of the structure observed in both  $(\gamma, n)$  and  $(\gamma, p)$  reactions in  $O^{16}$ .

Groups A, B, and C of Fig. 6 could result either from transitions to excited states of  $N^{15}$  at 5.3-, 6.3-, and 7.3-Mev excitation, or from absorption of photons of lesser energy and subsequent decay to the ground state of  $N^{15}$ . Again, evidence from other experiments aids in assigning these proton groups. Spicer<sup>7</sup> has observed an absorption resonance in oxygen at about 14.7 Mev which has been ascribed to electric quadrupole absorption.<sup>24</sup> Protons from this resonance would contribute to group A. Our observation of approximate isotropy for protons of group A is consistent with a superposition of Spicer's observed  $(1 + \cos^2\theta)$  angular distribution and a  $(1 + \sin^2\theta)$  distribution which might be expected for  $p$  protons resulting from transitions between a  $1^-$  giant resonance state in  $O^{16}$  and the  $\frac{3}{2}^+$  state in  $N^{15}$  at 7.3 Mev (or a tail of the 6.3-Mev state).

Recently reported measurements of gamma rays emitted in the photodisintegration of oxygen<sup>25</sup> indicate a predominance of 6.3-Mev gammas associated with  $O^{16}(\gamma, p)$  and  $O^{16}(\gamma, n)$ . This appears to be evidence for

assigning a large probability to transitions to the  $\frac{3}{2}^-$  state at 6.3 Mev compared with transitions to the states at 5.3 and 7.3 Mev, and makes it likely that group B is due to these favored transitions. The origin of the remaining group C, is uncertain. It may arise in part from transitions to the 6.3-Mev state and in part from photon absorption by a level in  $O^{16}$  near 17 Mev. The work of Johansson and Forlsman<sup>8</sup> suggests such a level but this is not substantiated by Spicer's measurements<sup>7</sup> in the same region.

The transitions from the  $1^-$  states of  $O^{16}$  to the  $\frac{1}{2}^-$  ground state of  $N^{15}$  can yield photoprotons with zero or two units of angular momentum. It might be expected that the  $d$  protons would be inhibited by the centrifugal barrier. The  $s$  protons should then give isotropic angular distribution. Yet we find these protons to have an angular distribution peaked near  $90^\circ$  as shown in Fig. 7, indicating appreciable enhancement of protons of nonzero angular momentum. A similar enhancement of  $d$  protons was observed in carbon.<sup>12</sup> A model which provides such an enhancement is the independent-particle model proposed by Wilkinson.<sup>26</sup> In this model the initial nucleus is considered to be well described by a shell model state. The excitation transitions allowed on the absorption of a photon are those in which no more than one nuclear particle changes its configuration. In particular, a proton from the last closed shell is elevated to an  $l+1$  shell by an electric dipole photon absorption. If this excited proton is emitted before interacting with the rest of the nucleus, it will of course carry  $l+1$  units of angular momentum away with it, leaving the resultant nucleus in a "parent" state. In the oxygen photoproton case, transitions should be probable only to those states in  $N^{15}$  which are "parents" of the ground state of oxygen. Since the transitions involve protons in the  $p_{\frac{1}{2}}$  or  $p_{\frac{3}{2}}$  shells of  $O^{16}$  excited to the  $d_{\frac{1}{2}}$  or  $d_{\frac{3}{2}}$  states in  $O^{16}$ , there are only two "parent" states in  $N^{15}$  on both  $jj$  and  $LS$  coupling, namely, the  $\frac{1}{2}^-$  ground state and  $\frac{3}{2}^-$  excited state (6.3 Mev) of  $N^{15}$ . As discussed above, the present oxygen data combined with Svantesson's<sup>25</sup> observations on the 6.3-Mev gamma ray are consistent with this model. However, the presence of several narrow, closely spaced absorption resonances<sup>27</sup> seems to indicate strong mixing between states involving single-particle excitation and those in which the excitation energy is shared among several particles.

<sup>23</sup> A. S. Penfold and B. M. Spicer, Phys. Rev. **100**, 1377 (1955).

<sup>24</sup> D. H. Wilkinson, Phys. Rev. **99**, 1347 (1955).

<sup>25</sup> N. Svantesson, Bull. Am. Phys. Soc. Ser. II, **1**, 28 (1956), private communications from E. Fuller and E. Hayward.

<sup>26</sup> D. H. Wilkinson, *Proceedings of the 1954 Glasgow Conference on Nuclear and Meson Physics* (Pergamon Press, London, 1955), p. 161.

<sup>27</sup> Also known from  $(\gamma, n)$  work at Saskatchewan and Illinois (see reference 9).